SLAC-PUB-1293
(A)
August 1973

CURRENT INJECTION AND COLLECTION IN A RECTANGULAR SUPERCONDUCTOR*

Héctor Moreno** and Mario Rabinowitz
Stanford Linear Accelerator Center
Stanford University, Stanford, California 94305

Abstract

A general two-dimensional analytical solution is presented for the problem of transport current injection from a normal conductor into a superconductor and collection back into a normal conductor. The current distribution is solved for the general case which takes in the full range from essentially point source to full-width injection and collection. The current distribution also represents that in a split ring superconductor joined by a link of variable width. A comparison is made with current injection into and collection from a normal conductor. Computer calculations are included showing a virtual anomaly which is reconciled. Speculation is made regarding the formation of transport current vortices in an initially simply-connected superconductor.

(Submitted for publication)

*Work supported by the U. S. Atomic Energy Commission.

** Fellow of Centro de Investigación y de Estudios Avanzados del IPN and Consejo Nacional de Ciencia y Tecnologiá (México).

I. Analysis of Injection and Collection in a Superconductor

With the increasing use of superconductors in electromagnets, in power transmission, and in electrical machinery, the normal to superconducting interface becomes a more scientifically and technologically important boundary to understand. It is of interest to consider the general case of current injection from a normal conductor into a superconductor and collection back into a normal conductor. The results are also valid for the current distribution in a superconducting split ring joined by a link of variable width. For generality, let the injection and collection regions be of arbitrary width 2d in a rectangular superconductor of width 2a and length 2b, as shown in Fig. 1. So that the problem may be treated two-dimensionally, the superconductor may be either a thin film or infinitely thick. The current, I, is homogeneous within the injection region of current density, $J = I/2d$, per unit length.

By taking the curl of the London equation

$$\nabla \times \left[\nabla \times \vec{j} = \frac{-1}{\mu \lambda^2} \vec{B} \right] , \tag{1}$$

and combining it with Maxwell's equation

$$\mu \vec{j} = \nabla \times \vec{B} \qquad \text{(no displacement current)} \tag{2}$$

and the continuity condition $\nabla \cdot \vec{j} = 0$ for steady state, we have

$$\nabla^2 \vec{j} = \frac{1}{\lambda^2} \vec{j} = \beta^2 \vec{j} \tag{3}$$

as the differential equation to solve to obtain the distribution of supercurrent density $\vec{j}$ in the superconductor. For convenience, we have defined β as the inverse of the penetration depth λ.

Due to the symmetry provided by our choice of coordinates, j_y and j_z, the components of $\vec{j}$ have the following symmetry properties to guide us in the solution of Eq. (3):

$$j_y(y, z) = -j_y(y, -z) = -j_y(-y, z) = j_y(-y, -z) \tag{4}$$

$$j_z(y, z) = j_z(y, -z) = j_z(-y, z) = j_z(-y, -z) \quad . \tag{5}$$

The boundary conditions are given by:

$$j_y(\pm a, z) = 0 \tag{6}$$

$$j_z(y, \pm b) = J\left\{\theta(y+d) - \theta(y-d)\right\} = \begin{cases} J & -d < y < d \\ 0 & \text{otherwise} \end{cases} , \tag{7}$$

where θ is the unit step function.
Assuming separation of variables, $j_y = g(y)\,h(z)$, then Eq. (3) (which holds for j_y and j_z as well as $\vec{j}$) yields

$$\frac{1}{g}\frac{d^2 g}{dy^2} + \frac{1}{h}\frac{d^2 h}{dz^2} - \beta^2 = 0 \quad . \tag{8}$$

Using the boundary condition (6), Eq. (8) separates thus

$$\frac{d^2 g(y)}{dy^2} + \eta^2 g(y) = 0 , \tag{9}$$

and

$$\frac{d^2 h(z)}{dz^2} - (\beta^2 + \eta^2)\,h(z) = 0 \quad , \tag{10}$$

where $\eta^2 > 0$ is the separation constant.

Equation (9) has a solution of the form $g(y) \propto \sin \eta y$ and Eq. (10) implies $h(z) \propto \sinh \left[\beta^2 + \eta^2\right]^{1/2} z$, where

$$\eta = \frac{n\pi}{a} , \quad n = 1, 2, 3, \ldots \quad . \tag{11}$$

Hence the general solution to Eq. (3) for j_y is

$$j_y = \sum_{n=1}^{\infty} - A_n \sin\left(\frac{n\pi}{a} y\right) \sinh\left[\beta^2 + \left(\frac{n\pi}{a}\right)^2\right]^{1/2} z \quad , \tag{12}$$

where the coefficients A_n have yet to be determined.

To determine j_z, one may proceed similarly as above, or use the continuity equat ion

$$\frac{\partial j_z}{\partial z} = \frac{-\partial j_y}{\partial y} = \sum_{n=1}^{\infty} A_n\left(\frac{n\pi}{a}\right)\cos\left(\frac{n\pi}{a} y\right) \sinh\left[\beta^2 + \left(\frac{n\pi}{a}\right)^2\right]^{1/2} z \tag{13}$$

which relates j_z to j_y. Thus, by simple integration of (13), we have

$$j_z = \sum_{n=1}^{\infty} \frac{\pi n A_n}{\left[(\beta a)^2 + (n\pi)^2\right]^{1/2}} \cos\left(\frac{n\pi}{a} y\right) \cosh\left[\beta^2 + \left(\frac{n\pi}{a}\right)^2\right]^{1/2} z + f(y) \ , \tag{14}$$

since $\frac{\partial f(y)}{\partial z} = 0$. $f(y) = f(-y)$ is a solution of $\nabla^2 f = \beta^2 f$. Thus

$$f(y) = A \cosh \beta y \ , \tag{15}$$

where A and the A_n coefficients may be determined by the boundary condition (7). Thus

$$A = \frac{J \int_{-d}^{d} dy}{\int_{-a}^{a} \cosh \beta y \, dy} = \frac{J d \beta}{\sinh \beta a} \ , \tag{16}$$

and

$$A_n = \frac{-A \int_{-a}^{a} \cos\left(\frac{n\pi y}{a}\right)\cosh\beta y \, dy + J \int_{-d}^{d} \cos \frac{n\pi y}{a} dy}{\frac{n\pi a}{\left[(\beta a)^2 + (n\pi)^2\right]^{1/2}} \cosh b \left[\beta^2 + \left(\frac{n\pi}{a}\right)^2\right]^{1/2}}$$

$$= \frac{2J\left[(\beta a)^2 + (n\pi)^2\right]^{1/2} \sin\left(\frac{n\pi d}{a}\right)}{(n\pi)^2 \cosh b \left[\beta^2 + \left(\frac{n\pi}{a}\right)^2\right]^{1/2}} - \frac{(-1)^n \, 2Jd(\beta a)^2}{n\pi a\left[(\beta a)^2 + (n\pi)^2\right]^{1/2} \cosh b\left[\beta^2 + \left(\frac{n\pi}{a}\right)^2\right]^{1/2}} \, . \tag{17}$$

A. Full Width Injection

If we take d = a, this corresponds to full width injection, and we can easily compare our results with London's[1] calculation, as we have used the same symbols for this purpose. In this case, the first term in (17) is 0 and Eq. (12) becomes

$$j_y = \sum_{n=1}^{\infty} \frac{(-1)^n 2J(\beta a)^2 \sin\left(\frac{n\pi}{a} y\right) \sinh\left[\beta^2 + \left(\frac{n\pi}{a}\right)^2\right]^{1/2} z}{n\pi\left[(\beta a)^2 + (n\pi)^2\right]^{1/2} \cosh b\left[\beta^2 + \left(\frac{n\pi}{a}\right)^2\right]^{1/2}} \, . \tag{18}$$

Equation (14) becomes

$$j_z = \frac{J\beta a \cosh\beta y}{\sinh\beta a} - \sum_{n=1}^{\infty} \frac{(-1)^n 2J(\beta a)^2 \cos\left(\frac{n\pi}{a} y\right) \cosh\left[\beta^2 + \left(\frac{n\pi}{a}\right)^2\right]^{1/2} z}{\left[(\beta a)^2 + (n\pi)^2\right] \cosh b\left[\beta^2 + \left(\frac{n\pi}{a}\right)^2\right]^{1/2}} \, . \tag{19}$$

Our results differ from those of London[1]; however, we ascribe this to typographical errors in London's book. The differences are: In Eq. (18) London's summation for j_y (p. 40) is negative whereas ours is positive. In Eq. (19) for j_z

London (p. 40) has a positive sum whereas ours is negative. In addition, he has $\left[(\beta a)^2 + (n\pi)^2\right]^{1/2}$, while we have no square root for this factor. We have $\cosh\left[\beta^2 + \left(\frac{n\pi}{a}\right)^2\right]^{1/2} b$ in the denominator whereas he has sinh. Otherwise for this case the results are the same.

B. Point Injection

It is interesting to look at the opposite limit, which is the other extreme for d. The limit $d \to 0$, with $J \to \infty$ and $2dJ \to I$ = the injection current, represents the limit of point injection and collection. In this case, we have

$$j_y = \frac{-I}{\pi a} \sum_{n=1}^{\infty} \left[\frac{\left[(\beta a)^2 + (n\pi)^2\right]^{1/2}}{n \cosh b \left[\beta^2 + \left(\frac{n\pi}{a}\right)^2\right]^{1/2}} - \frac{(-1)^n (\beta a)^2}{n\left[(\beta a)^2 + (n\pi)^2\right]^{1/2} \cosh b \left[\beta^2 + \left(\frac{n\pi}{a}\right)^2\right]^{1/2}} \right] \cdot$$

$$\sin\left(\frac{n\pi}{a} y\right) \sinh\left[\beta^2 + \left(\frac{n\pi}{a}\right)^2\right]^{1/2} z \quad . \tag{20}$$

$$j_z = \frac{I\beta \cosh \beta y}{2 \sinh \beta a} + I \sum_{n=1}^{\infty} \left\{ \frac{1}{a \cosh b \left[\beta^2 + \left(\frac{n\pi}{a}\right)^2\right]^{1/2}} \left[1 - \frac{(-1)^n (\beta a)^2}{\left[(\beta a)^2 + (n\pi)^2\right]} \right] \right\} \cdot$$

$$\cos\left(\frac{n\pi}{a} y\right) \cosh\left[\beta^2 + \left(\frac{n\pi}{a}\right)^2\right]^{1/2} z \quad . \tag{21}$$

II. Computer Results for the Super-current

Equations (12) and (14) were programmed for computer calculation so that the streamlines showing the current distribution could be plotted. Thus the path taken by a given current line can easily be followed by this visualization. Either of two approaches can be taken, both of which start with the calculation of j_{y1} and j_{z1} at the point (y_1, z_1).

These components of $\vec{j}$ can then be converted into velocity components v_{y1} and v_{z1} by dividing by the electron number density and charge. Then, by taking a small time interval t, the next point the electrons move to is found from $y_2 = v_{y2} t + y_1$ and $z_2 = v_{z2} t + z_1$. j_{y2} and j_{z2} are then calculated, and by repeating the process, the entire electron trajectory or streamlines are calculated. Another approach is to take the normalized current density vector $\vec{j}/\left(j_y^2 + j_z^2\right)^{1/2}$, times a small constant interval in obtaining the next point (y_2, z_2), etc. The difference between the two approaches is that the former involves a variable step size, whereas the latter step size is constant. The former approach gives a more accurate representation. However, for our purposes, the difference in accuracy is not substantial, and the latter method was used for convenience. The results of three calculations are illustrated in Fig. 2, 3, and 4. Only a portion of the first quadrant is shown, as the streamlines in the other quadrants may be found by mirror symmetry.

Figure 2 shows three streamlines for $a = b = 5\lambda = 5/\beta = 100d$, using 50 harmonics. ($\lambda$ was chosen not too small compared with a and b so that it would be easy to illustrate the streamlines.) This could represent a small square plate with current injection and collection by means of fine wires or whiskers, or a point-link split-ring superconductor. Streamlines I and II are nicely behaved, as they appear smoothly varying. Streamline III shows an oscillatory behavior near the boundary $z = b$.

Figure 3 shows streamline III together with two more streamlines IV and V even closer to the $z = b$ boundary, also using 50 harmonics. Streamline IV has a slightly higher oscillation amplitude than III, and V has the highest. Thus we see that the oscillation amplitude increases as a given streamline is closer to $z = b$. The amplitude also increases as the injection region is approached, as well as when $y \rightarrow a$, as illustrated by streamline V. This behavior can be interpreted as a Gibbs overshoot. We interpret the oscillation near $z = \pm b$ as a lack of accuracy in the boundary condition representation due to the limited number of harmonics.

This interpretation was tested by decreasing the number of harmonics from 50 to 25 in the calculation. As expected, the oscillation increased accordingly. This case is depicted in Fig. 4 where the streamline shown corresponds to streamline III of the previous figures. The oscillation should not be present in the actual experimental situation of homogeneous current injection and collection within the region $-d < y < d$. It arises due to the harmonic series representation, and would vanish as $n \rightarrow \infty$ (except for the Gibbs overshoot).

III. Current Injection and Collection in a Normal Conductor

The differential equations describing the current distribution in a normal conductor resulting from a given configuration of injection and collection may be obtained from Maxwell's equations and Ohm's law by a method similar to that of Section I. However the same result may now be obtained more easily by noting that as $\beta \rightarrow 0$ (penetration depth $\lambda \rightarrow \infty$) this limit corresponds to the passage from the superconducting to the normal state. Hence we may use Eqs. (12) and (14) with $\beta \rightarrow 0$ for the case of a normal conductor. The results of the computer calculation for this case are displayed in Fig. 5, where streamlines I_N, II_N, and III_N are shown. These streamlines correspond to I, II, and III of the superconducting case (Fig. 2) in that they pass through the same points on the $z = 0$ line, namely at $y = 0.99$, 0.96, and 0.93 respectively.

The behavior of the streamlines in the normal state as contrasted with the superconducting state is that they penetrate the film surface more, as is to be expected. Thus, there is not a sharp turn near the corner for III_N and this streamline does not manifest the Gibbs overshoot phenomenon in that region. (However, a streamline much closer to the corner should show a Gibbs overshoot for the normal case similar to that observed for the superconductor.) Otherwise the oscillatory pattern and the behavior near the injection and collection regions is similar to the superconducting case.

IV. Discussion

The interesting observation of representational spatial oscillation of the current near $z = \pm b$ made in Sections II and III, and depicted in Figs. 2, 3, 4 and 5 raises the question as to what experimental conditions would in fact give rise to an actual spatial current oscillation. An obvious configuration would be an undulating boundary. A superconductor with dimensions large with respect to λ would impart this oscillation to a larger fraction of the current due to the confinement of most of the current within the penetration depth λ, as compared to a normal conductor.

An experimental configuration which more closely simulates the analysis with a limited number of harmonics is that of a discrete number of small injection and collection regions distributed over the width of the superconductor. This may even arise inadvertently when a normal conductor makes poor contact with a superconductor at the interface. Such a situation leads to a stimulating speculation: Can a proper configuration of injection and collection points be realized which would lead to vortex formation in the current distribution in an initially simply-connected superconductor? Heuristically it would seem possible by setting up the injection and collection points to give the proper magnitude and asymmetry to the oscillation in the transport current. In this case the same results should be obtained experimentally and theoretically.

A fluid flow analogue to the supercurrent distribution obtained in Section II, is that of the point injection and collection of gas into a cylinder with blocking horns as shown in Fig. 6. In this case it is possible to experimentally set up turbulent flow giving rise to vortices. This might lead one to think that it should similarly be possible to obtain vortices in a superconductor using single point injection and collection regions. It remains a problem for experimental determination as to whether or not vortices can thus be created. This question may be of interest in dealing with the phenomenology of Josephson junctions, since they may be understood as superconducting rings with self point injection and collection of current.

A physically significant and interesting process occurs as the current density is increased by increasing the current or as the injection and collection regions are reduced in size while a constant current is maintained. A point may be reached where the self-magnetic field of the transport current would exceed the effective critical field of the superconductor thus creating a normal region in the superconductor near the injection region. The current would then go straight in as well as being confined near the boundary. Under certain conditions this could lead to an oscillation of this region between the normal and superconducting states. Vortices could well form under these circumstances.

Morgan[2] has recently calculated the eddy currents induced in flat metal-filled superconducting braids by a time varying magnetic field. He considers the field distortions caused by eddy currents in the braid. We wish to point out another possible contribution to undesirable field shape changes related to our analysis. The superconductor is usually in intimate contact throughout with a good normal conductor such as copper to produce superior electrical stability and mechanical properties. However the eddy currents induced in the normal metal, may act as injection and collection points into and from the superconductor. In some cases this change in the current distribution in the superconductor itself may contribute non-negligibly to the field distortion.

V. Acknowledgments

We wish to thank David Frankel for making initial computer calculations, and David Slone for helpful discussions regarding the normal conductor. Thanks are also due to Dr. Edward Garwin for his interest in the problem and his useful comments. One of us (HM) is grateful to the Centro de Investigación y de Estudios Avanzados del IPN and the Consejo Nacional de Ciencia y Tecnología of México for their financial support.

References

1. F. London, Superfluids Volume I, Macroscopic Theory of Superconductivity (Dover Publications, Inc., New York, 1960) Section 4.

2. G. H. Morgan, J. Appl. Phys. 44, 3319 (1973).

Figure Captions

1. Rectangular superconductor showing current injection and collection regions.
2. Three computed streamlines for $a = b = 5\lambda = 100d$, using 50 harmonics.
3. Streamline III, together with two more streamlines IV and V, also using $a = b = 5\lambda = 100d$, and 50 harmonics.
4. Increase in oscillation amplitude of the streamline corresponding to III due to a decrease in the number of harmonics to 25.
5. Three streamlines in a normal conductor corresponding to the three in Fig. 2.
6. Schematic representation of vortex formation in turbulent fluid flow.

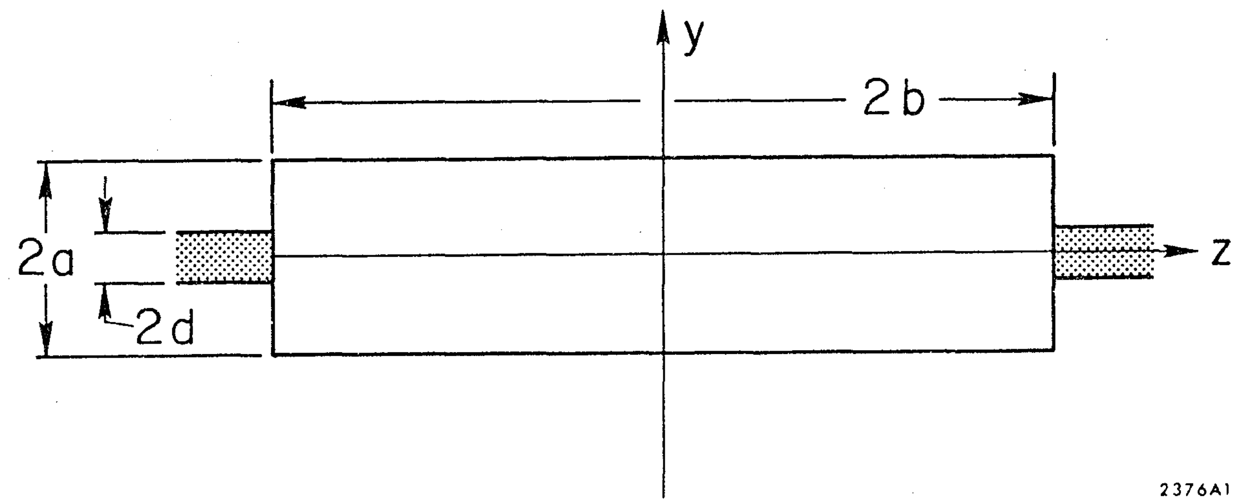

Fig. 1

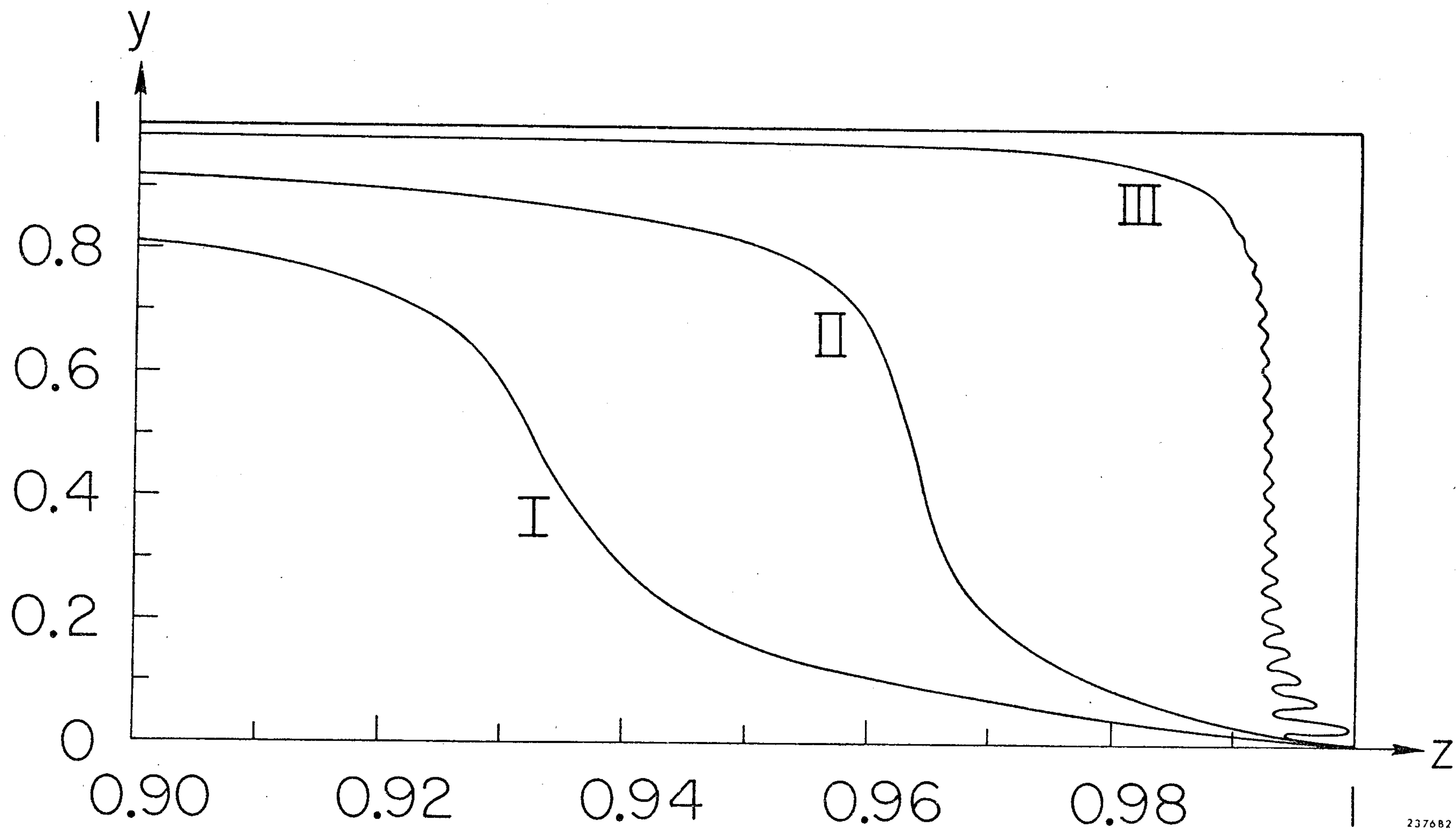

Fig. 2

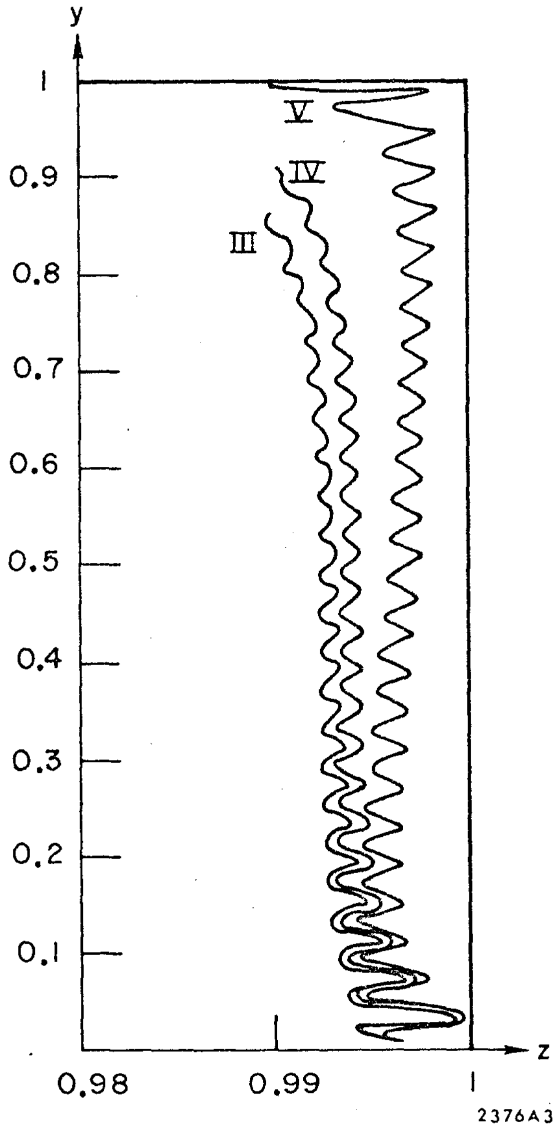

Fig. 3

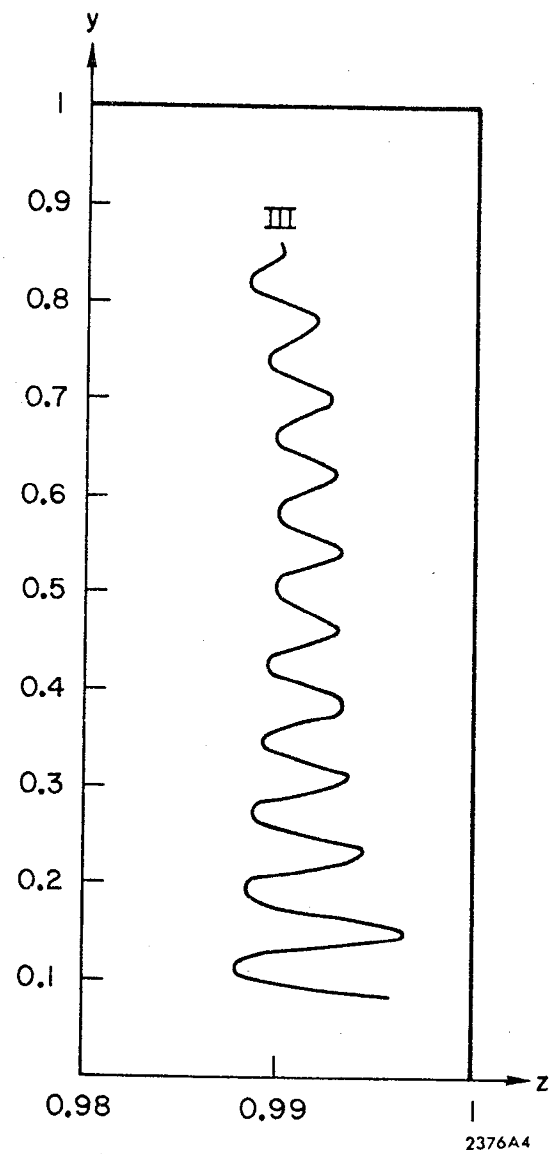

Fig. 4

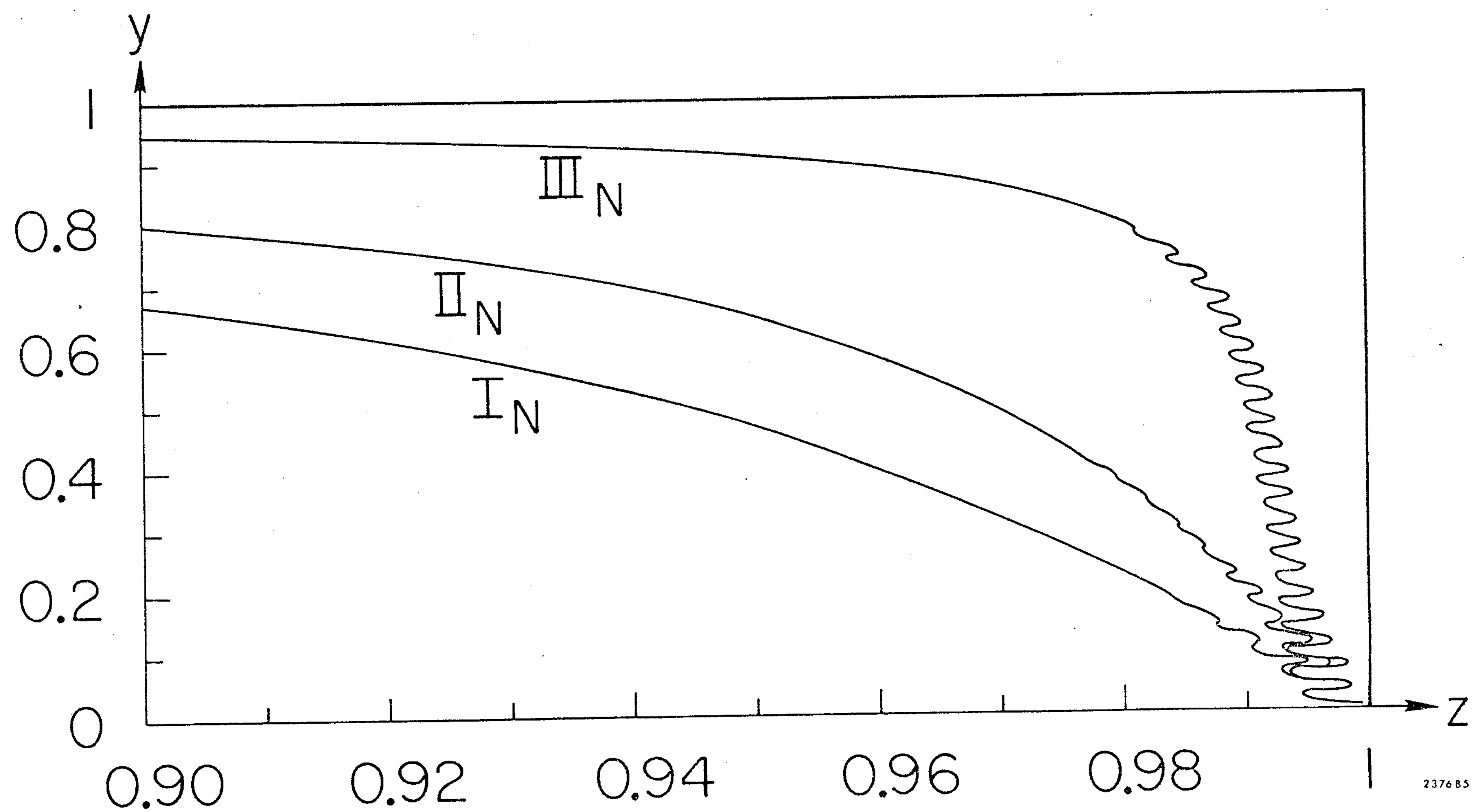

Fig. 5

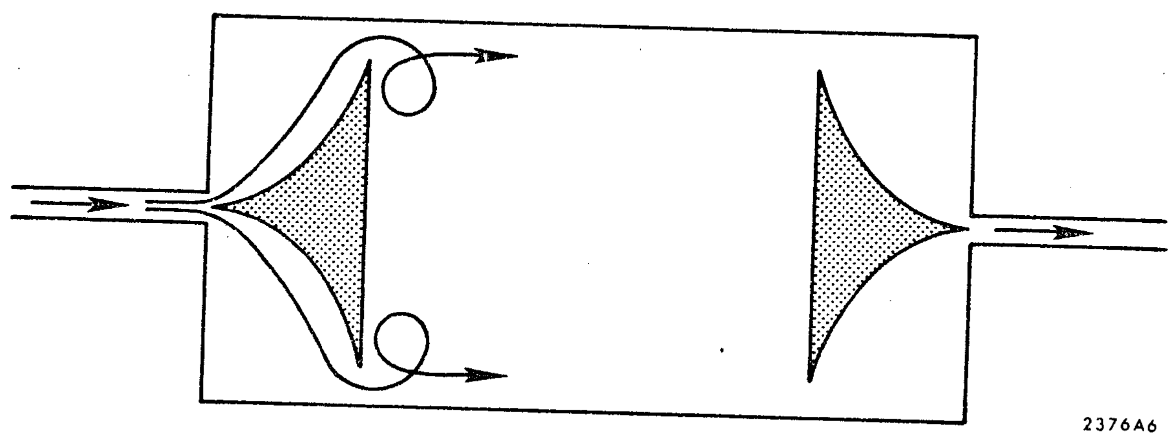

2376A6

Fig. 6